


Quantum-Classical Correspondence of Non-Hermitian Symmetry Breaking

Zhuo-Ting Cai, Hai-Dong Li, and Wei Chen  *

*National Laboratory of Solid State Microstructures,
School of Physics, Jiangsu Physical Science Research Center,
and Collaborative Innovation Center of Advanced Microstructures, Nanjing University, Nanjing 210093, China*
(Dated: November 27, 2024)

Real-to-complex spectral transitions and the associated spontaneous symmetry breaking of eigenstates are central to non-Hermitian physics, yet their underlying physical mechanisms remain elusive. Here, we resolve the mystery by employing the complex path integral formalism and developing a generalized Gutzwiller trace formula. These methodologies enable us to establish a universal quantum-classical correspondence that precisely links the real or complex nature of individual energy levels to the symmetry properties of their corresponding semiclassical orbits. Specifically, in systems with a general η -pseudo-Hermitian symmetry, real energy levels are quantized along periodic orbits that preserve the corresponding classical S_η symmetry. In contrast, complex conjugate energy levels arise from semiclassical orbits that individually break the S_η symmetry but together form S_η -symmetric pairs. This framework provides a unified explanation for the spectral behaviors in various continuous non-Hermitian models and for the \mathcal{PT} transition in two-level systems. Our work uncovers the physical mechanism of non-Hermitian symmetry breaking and introduces a new perspective with broad implications for the control and application of non-Hermitian phenomena.

Introduction.—In the past decade, great research progress has been made in non-Hermitian physics [1–3]. Different from the standard quantum mechanism in which the Hamiltonian of a closed system is represented by a Hermitian operator, non-Hermitian Hamiltonians can effectively describe various physical effects in open systems. Recently, numerous interesting non-Hermitian phenomena have been discovered, such as the non-Hermitian spectral phase transitions [4–19], novel physics associated with exceptional points [20–23], the non-Hermitian skin effect [24–29] and the non-reciprocal phase transitions [30], which not only deepen our understanding of the physical world but may also lead to interesting applications [31–37]. These non-Hermitian effects are directly attributable to, or closely linked with, the properties of the non-Hermitian energy spectra and the corresponding eigenstates, which constitute the main focus of non-Hermitian physics.

In contrast to the Hermitian Hamiltonian that ensures an entirely real energy spectrum, non-Hermitian systems exhibit richer spectral characteristics. For the most relevant class of non-Hermitian Hamiltonians that satisfy the condition of pseudo-Hermiticity [2, 38], their energy levels are either real or appear as complex conjugate pairs. A notable example is the parity-time (\mathcal{PT}) transition [4], where variation in model parameters can drive a real-to-complex spectral transition, accompanied by spontaneous symmetry breaking of the corresponding eigenstates. These non-Hermitian phenomena have been known for a long time with their validity grounded in mathematical theorems [39] and confirmed by experiments [5–10]. However, unlike the spontaneous symmetry breaking in conventional phase transitions stabilized by the principle of lowest free energy, the non-Hermitian

spectral transitions and symmetry breaking just take place naturally as the model parameters vary. Whether a fundamental and universal mechanism exists governing these phenomena remains an open question. Answering this question can not only enhance our comprehension of non-Hermitian phenomena but also provide practical insights for their control.

In this Letter, we provide an affirmative answer to this question by developing a general theory of non-Hermitian symmetry breaking. In particular, we establish a quantum-classical correspondence between the properties of individual energy levels and the symmetry of their corresponding semiclassical orbits, as illustrated in Fig. 1. This correspondence is achieved by employing the complex path integral approach and deriving a generalized Gutzwiller trace formula for a broad class of analytic non-Hermitian problems exhibiting pseudo-Hermiticity. We demonstrate that any η -pseudo-Hermitian symmetry (η -PHS) (Eq. (1), defined for the quantum Hamiltonian) leads to a corresponding semiclassical S_η symmetry (Eq. (4), defined for the corresponding classical Hamiltonian). The trace formula quantizes each energy level along periodic orbits in complex spacetime, and the symmetry properties of the orbits dictate whether the energy level is real or complex. Specifically, a real energy level E_n occurs as the semiclassical orbit O possesses the S_η symmetry. Otherwise, complex conjugate energy pairs, denoted as $E_{n1} = E_{n2}^*$, arise when the corresponding orbits O_1 and O_2 individually break the S_η symmetry but collectively form an S_η -symmetric pair [cf. Fig 1]. The validity and universality of our theory are confirmed through its application to various continuous non-Hermitian models and the \mathcal{PT} transition in two-level systems.

Quantum-classical correspondence of symmetry.— We first investigate a general non-Hermitian Hamiltonian $\mathcal{H}(\hat{x}, \hat{p})$ with a continuous energy spectrum, where \hat{x} and

* Corresponding author: pchenweis@gmail.com

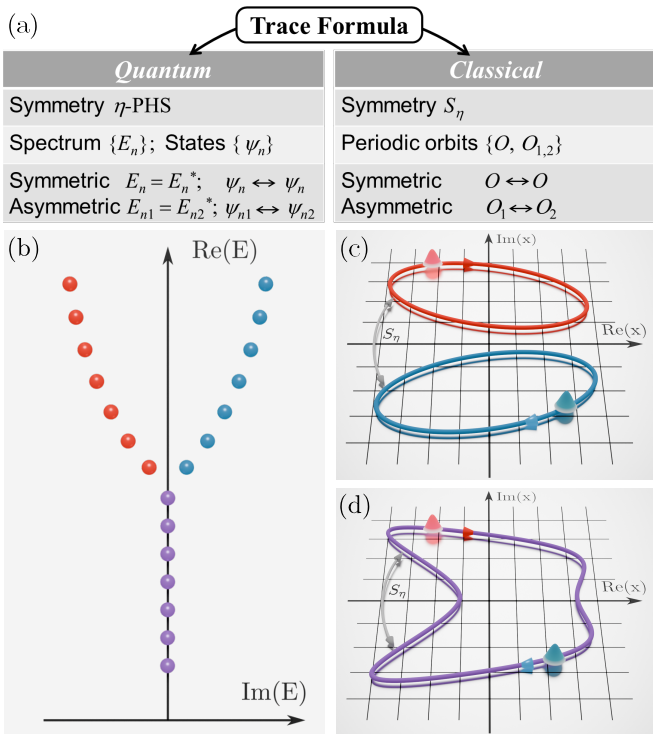


FIG. 1. Quantum-semiclassical correspondence of non-Hermitian physics. (a) Quantum and classical properties are related by the trace formula. (b-d) Schematic diagrams illustrating the correspondence between non-Hermitian energy spectrum and semiclassical orbits of wave packets. (b) Energy spectrum consisting of real parts and complex conjugate pairs represented by colored balls. (c) Two semiclassical orbits in complex coordinate space forming an S_η -symmetric pair, corresponding to the complex energy pairs. (d) An S_η -symmetric orbit corresponding to real eigenenergies. The eigenenergies and the corresponding orbits are indicated by the same colors. The S_η symmetry operation is denoted by the gray bidirectional arrows.

\hat{p} denote the coordinate and momentum operators, respectively. Non-Hermitian Hamiltonians that satisfy the condition of η -pseudo-Hermiticity [38] are of particular interest:

$$\eta \mathcal{H}(\hat{x}, \hat{p}) \eta^{-1} = \mathcal{H}^\dagger(\hat{x}, \hat{p}), \quad (1)$$

where $\eta = \eta^\dagger$ is a general invertible Hermitian operator. This constraint, referred to as η -PHS, plays a critical role in shaping the energy spectrum, with its preservation or breaking strongly influencing the spectral properties [39].

To establish the connection between quantum and semiclassical pictures in Fig. 1, we start with the propagator $G(x_f, x_i, t) = \langle x_f | e^{-i\mathcal{H}t} | x_i \rangle$ from x_i to x_f in coordinate space ($\hbar = 1$ is taken). For later purposes, all physical quantities, including coordinates, momenta, and time, are considered to be complex [40–42]. It means that $G(x_f, x_i, t)$ is expressed under the biorthonormal eigenbasis of \hat{x} . The η -PHS (1) imposes the following

constraint on the propagator [43]

$$G_\eta(x_f, x_i, t) = G^*(x_i^*, x_f^*, -t^*), \quad (2)$$

where $G_\eta(x_f, x_i, t) = \langle x_f | e^{-i\mathcal{H}(\hat{x}_\eta, \hat{p}_\eta)t} | x_i \rangle$ with $\hat{x}_\eta = \eta \hat{x} \eta^{-1}$, $\hat{p}_\eta = \eta \hat{p} \eta^{-1}$, and $G^*(x_i^*, x_f^*, -t^*) = [\langle x_i | e^{i\mathcal{H}(\hat{x}^\dagger, \hat{p}^\dagger)t^*} | x_f \rangle]^*$. Such a constraint indicates that any specific η -PHS corresponds to a classical symmetry S_η . To this end, we express the propagator in terms of the path integral in phase space and Eq. (2) leads to

$$\int_{x_i}^{x_f} \mathcal{D}[\xi] e^{i \int_0^t [p\dot{x} - H(x_\eta, p_\eta)] dt'} = \int_{x_i}^{x_f} \mathcal{D}[\xi] e^{i \int_0^t [p\dot{x} - H^*(x^*, p^*)] dt'}, \quad (3)$$

where $\xi(t) := \{x(t), p(t)\}$ denotes the phase space coordinate, the integrations over x , p and t' are along certain paths in the respective complex planes, and $x_\eta = x_\eta(x, p)$, $p_\eta = p_\eta(x, p)$ are both functions of x, p [43]. In the path integral formula, the coordinates, momenta and thus the Hamiltonian H all become c-numbers. Eq. (3) holds for arbitrary values of x_i, x_f and t , indicating that the semiclassical Hamiltonian must adhere to the following constraint or, referred to as the S_η symmetry

$$S_\eta : H(x_\eta, p_\eta) = H^*(x^*, p^*), \quad (4)$$

which is the semiclassical counterpart of the η -PHS. The S_η symmetry governs the semiclassical dynamics of the system and will be inherited by the classical orbits.

Generalized Gutzwiller trace formula.—The energy spectrum of \mathcal{H} corresponds to the poles of the trace of the Green's operator $G(E) = \text{Tr}(\mathcal{H} - E)^{-1}$. This conclusion applies to both real and complex energy values, indicating that the energy spectrum of both Hermitian and non-Hermitian systems can be analyzed in the same way. In the Hermitian regime, the Gutzwiller trace formula expresses $G(E)$ in terms of the contour integral over periodic orbits so as to establish a connection between the energy spectrum and these semiclassical orbits [44]. We demonstrate that, by generalizing the Gutzwiller trace formula to the non-Hermitian regime, the long-standing puzzle of the underlying scenario for non-Hermitian spectral properties and symmetry breaking of eigenstates can be resolved through the semiclassical perspective.

Interpreting $G(E)$ as the Fourier transform of the time-domain propagator with the trace conducted in the coordinate space yields the complex path integral formula

$$G(E) = i \int dt e^{iEt} \int dx_i \int_{x_i}^{x_i} \mathcal{D}[\xi] e^{i \int_0^t [p\dot{x} - H(x, p)] dt'}. \quad (5)$$

We extend the conventional Gutzwiller trace formula to the non-Hermitian regime by repeatedly applying saddle point approximation (SPA) [45] to the complex path integral, instead of the stationary phase approximation in the Hermitian regime [43]. First, applying SPA to $\int_{x_i}^{x_i} \mathcal{D}[\xi]$ reduces the path integral to the contributions by those closed orbits obeying the complex Hamilton's

canonical equations $\dot{x} = \partial H / \partial p$, $\dot{p} = -\partial H / \partial x$. Second, SPA applied to $\int dx_i$ selects out the periodic orbits with identical initial and final momenta at x_i , including both their real and imaginary parts. Finally, SPA applied to $\int dt$ establishes the relation function $E = E(T)$ between energy E and periodicity T of the classical motion. In the non-Hermitian regime, periodic orbits may not exist when the periodicity T is restricted to be real [41]. To obtain periodic orbits, a complex T should be generally assumed [42]. The time-evolution contour lies in the complex t -plane that connects 0 and T . Although there are an infinite number of such contours, the evaluation of $G(x_i, x_i, T)$ does not rely on the specific choice of the contour [40]. Therefore, by choosing a proper time contour, $G(E)$ and the spectrum can be determined without ambiguity. After three steps of SPAs, we arrive at the trace formula involving contour integrals along all periodic orbits O as [43]

$$G(E) = iT(E) \frac{e^{i(\oint_O p dx - 2\pi\mu)}}{1 - e^{i(\oint_O p dx - 2\pi\mu)}}, \quad (6)$$

where $T(E)$ is the periodicity of the orbit for a given energy E and -4μ defines the Maslov index [46]. Extending the formula to more general cases involving distinct categories of periodic orbits is straightforward [43]. Although Eq. (6) possesses the same form as that in the Hermitian regime [44], the key distinction is that all physical quantities now reside in the complex domain. Poles of Eq. (6) correspond to the quantization condition in complex spacetime as

$$\oint_O p dx = (n + \mu)2\pi, \quad (7)$$

which determines the eigenenergies of the system. From Eq. (6), one can understand that the imaginary part of $\oint_O p dx$ represents the growth or decay of wave over one propagating cycle, while its real part represents the accumulated phase. Therefore, the quantization condition (7) determines the eigenenergies by selecting periodic orbits that exhibit quantized phase accumulations while maintaining a constant amplitude.

Semiclassical interpretation of non-Hermitian spectrum.—We have established the quantum-classical correspondence of symmetries (η -PHS $\leftrightarrow S_\eta$ as shown in Fig. 1) and interpreted non-Hermitian energy levels by quantized semiclassical orbits. Now we prove that the real or complex nature of each energy level is precisely determined by the S_η -symmetric properties of the corresponding periodic orbits. Physically, the semiclassical symmetry S_η in Eq. (4) implies that [43]

(i) If $\xi_1(t) = \xi(t)$ is a solution of the canonical equation, $\xi_2(t^*) = \xi_\eta(\xi^*(\mp t))$ is also a solution but along the time contour t^* , the two being S_η -symmetric to each other, where the “ \mp ” corresponds to whether the η operation involves a transpose or not.

Moreover, for periodic orbits $O_1(t)$ and $O_2(t^*)$ forming S_η -symmetric pairs, the following conclusions can be proved:

(ii) Their contour integrals satisfy the equality

$$\oint_{O_2(t^*)} p_2(t^*) dx_2(t^*) = \left(\oint_{O_1(t)} p_1(t) dx_1(t) \right)^*, \quad (8)$$

(iii) The energies and periods of O_1 and O_2 are complex conjugates:

$$E_1 = E_2^*, \quad T_1(E_1) = T_2^*(E_2). \quad (9)$$

The combination of these properties and the quantization condition can only yield two possible outcomes for nondegenerate eigenenergies [43]:

(1) O_1 and O_2 are essentially the same orbit obeying the S_η symmetry, and the quantized eigenenergies satisfying $E_n = E_n^*$, are real;

(2) O_1 and O_2 are different orbits related by the S_η operation ($S_\eta : O_1 \leftrightarrow O_2$), and the quantized eigenenergies constitute complex conjugate pairs with $E_{n1} = E_{n2}^*$.

Through this method, the non-Hermitian spectrum can be well interpreted by assigning a classical perspective to each energy level as sketched in Fig. 1. In the following, we use several concrete examples to verify the general conclusions obtained above and show the results collectively in Fig. 2. The main information conveyed by Fig. 2 is the quantum-classical correspondence between the energy spectrum properties and the symmetries of the corresponding orbits (more calculation details are provided in the Supplemental Material [43]).

Continuous systems.—First, we consider a continuous model $\mathcal{H}_1 = (\hat{p} + i\gamma)^2 + V(\hat{x})$ that exhibits non-Hermitian skin effect [24–29], where the real γ measures the strength of the skin effect and $V(\hat{x}) = V_0|\hat{x}|$ is a Hermitian potential. It possesses time-reversal (\mathcal{T}) symmetry with $\mathcal{H}_1 = \mathcal{T}\mathcal{H}_1\mathcal{T}^{-1} = \mathcal{H}_1^*$, which is equivalent to the T-PHS: $\mathcal{T}\mathcal{H}_1\mathcal{T}^{-1} = \mathcal{H}_1^\dagger$, with \mathcal{T} the transpose operation. Periodic boundary conditions are adopted in the calculations. We compare in Fig. 2(a1) the spectrum obtained by numerically solving the eigenvalue equation for \mathcal{H}_1 (with real x and $\hat{p} = -i\partial_x$) and that acquired via the generalized Gutzwiller trace formula using the quantization condition (7). The results from both methods demonstrate remarkable agreement, affirming the validity of our theory. The energy spectrum contains two distinctive parts, the one with real values and the remaining with complex conjugate pairs. Whether the eigenvalue is real or complex depends on the symmetry of the corresponding orbit. The S_η symmetry (4) of the semiclassical Hamiltonian is specified as $S_\mathcal{T} : H_1(x, -p) = H_1^*(x^*, p^*)$ in this case. This condition ensures that the solutions for periodic orbits, $O_1(t) = \{x(t), p(t)\}$ and $O_2(t^*) = \{x^*(-t), -p^*(-t)\}$, always form $S_\mathcal{T}$ -symmetric pairs. For every real energy level, the corresponding orbit obeys the $S_\mathcal{T}$ symmetry, as shown in Fig. 2(a2). In contrast, for any complex conjugate pair of energy levels, each of the corresponding orbits in phase space breaks the $S_\mathcal{T}$ symmetry. However, they are related to each other through the symmetry operation as $S_\mathcal{T} : O_1 \leftrightarrow O_2$, as illustrated

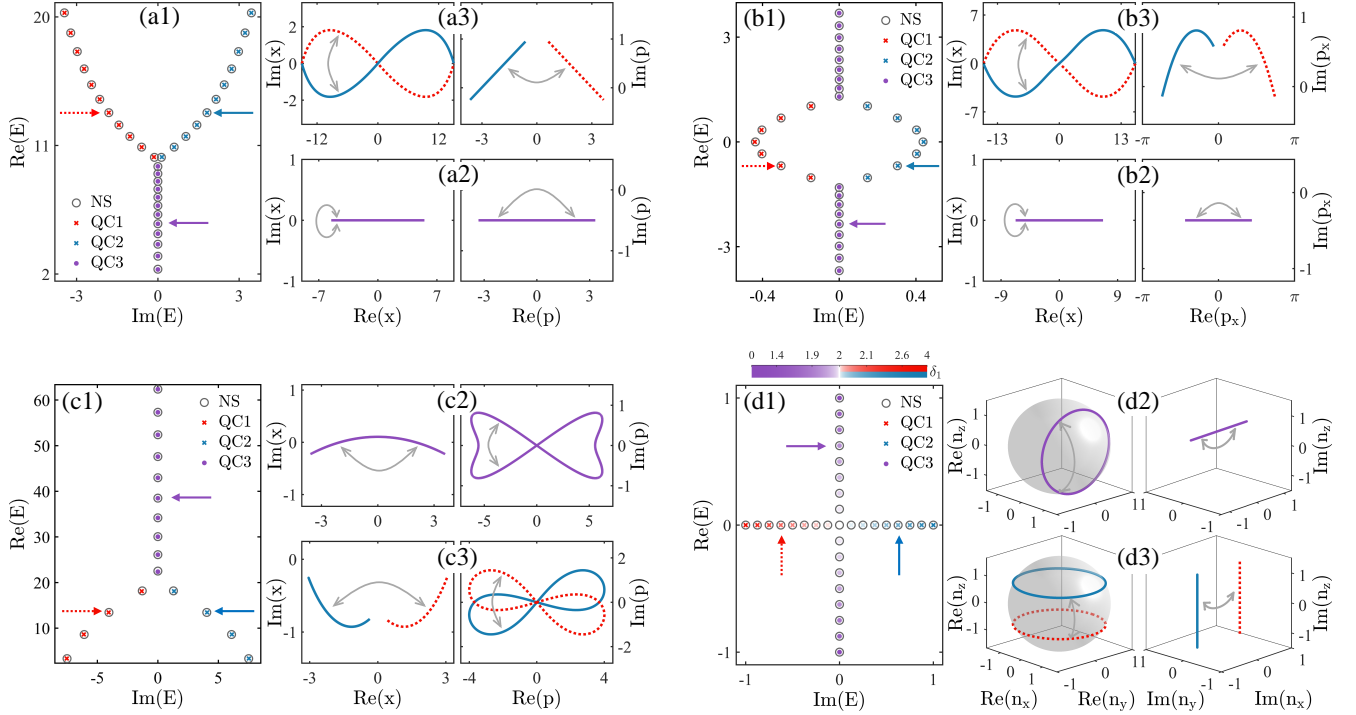


FIG. 2. Quantum-semiclassical correspondence validated by four concrete examples. (a1) Comparison between energy spectra obtained by numerical solutions (NS) of the eigenvalue equations of \mathcal{H}_1 and those solved by the quantization conditions (QC1, QC2, QC3) applied to different periodic orbits in (a2, a3). (a2) S_η -symmetric orbits in phase space corresponding to real eigenenergies in (a1). (a3) Asymmetric orbits in phase space constitute an S_η -symmetric pair corresponding to complex eigenenergies in (a1). The gray bidirectional arrows denote specific S_η symmetry operations. The results for $\mathcal{H}_2, \mathcal{H}_3$ and \mathcal{H}_4 are presented in the parallel way in (b1-b3), (c1-c3) and (d1-d3), respectively. (d1) Energy spectrum of the two-level system evolves with varying δ_1 . The relevant parameters are: (a1-a3) $\gamma = 0.5, V_0 = 1, L = 15$, (b1-b3) $t_0 = -1, \delta = 0.35, L = 32$, (c1-c3) $a = 2, g = 0.5, \Gamma = 4$, (d1-d3) $t_1 = 2$, where L denotes the scales of the systems.

by the gray bidirectional arrows in Fig. 2(a3). The results can be understood as follows. A particle with low energies is confined within the potential well with its orbit exhibiting the S_τ symmetry, resembling the situation for an open boundary condition. At high energies, the particle can overcome and traverse the potential barrier, which drastically changes the periodic orbit and break its symmetry. Two additional examples are investigated in parallel, with the results depicted in Figs. 2(b1-b3) and 2(c1-c3) respectively, both leading to the same conclusion. Detailed discussions can be found in the Appendix.

\mathcal{PT} transition in two-level systems.— Apart from continuous models, the non-Hermitian spectrum for discrete systems can also be interpreted within our framework. Take the \mathcal{PT} transition in the non-Hermitian two-level systems as an example, which has been extensively explored in optical systems with gain and loss [5–10]. It can be effectively captured by

$$\mathcal{H}_4 = \frac{1}{2} \mathbf{M} \cdot \boldsymbol{\sigma}, \quad \mathbf{M} = (t_1, 0, i\delta_1), \quad \boldsymbol{\sigma} = (\sigma_x, \sigma_y, \sigma_z), \quad (10)$$

where t_1 is the hopping, $i\delta_1$ describes the gain and loss for each level and $\boldsymbol{\sigma}$ is a vector composed of three Pauli ma-

trices $\sigma_{x,y,z}$. In optics, the two levels correspond to two different sites, which are interchanged under the parity operation $\mathcal{P} = \sigma_x$. Meanwhile, time reversal operation \mathcal{T} inverts the gain and loss. The system only obeys the combined \mathcal{PT} symmetry: $\mathcal{PT}\mathcal{H}_4(\mathcal{PT})^{-1} = \sigma_x \mathcal{H}_4^* \sigma_x = \mathcal{H}_4$, or the \mathcal{PT} -PHS: $\mathcal{PT}\mathcal{H}_4(\mathcal{PT})^{-1} = \mathcal{H}_4^\dagger$. The energy spectrum as a function of δ_1 , shown in Fig. 2(d1), remains real for $\delta_1 < t_1$ but becomes complex when $\delta_1 > t_1$. The spectral properties can be explained by the semiclassical (pseudo-)spin dynamics. For this purpose, we derive a similar trace formula for two-level systems applying the technique of spin path integral [43, 47, 48]. The corresponding semiclassical $S_{\mathcal{PT}}$ symmetry is expressed as

$$S_{\mathcal{PT}} : H_4(n_x, n_y, -n_z) = H_4^*(n_x^*, n_y^*, n_z^*), \quad (11)$$

where the vector $\mathbf{n} = (n_x, n_y, n_z)$ denotes the orientation of the classical spin. It dominates the classical equation of motion $\dot{\mathbf{n}} = \mathbf{M} \times \mathbf{n}$ and ensures the existence of two solutions $\mathbf{n}_1(t) = (n_x(t), n_y(t), n_z(t))$ and $\mathbf{n}_2(t^*) = (n_x^*(-t), n_y^*(-t), -n_z^*(-t))$ forming $S_{\mathcal{PT}}$ -symmetric pairs. When $\delta_1 < t_1$, the average spin vector during one period is aligned with $\pm \mathbf{M}$, and the periodic trajectories traced by its tip exhibit the $S_{\mathcal{PT}}$ symmetry;

see Fig. 2(d2). As δ_1 crosses t_1 , the classical trajectories of spin diverge to infinity, accompanied by an abrupt change in the direction of the average spin vector from $\pm\mathbf{M}$ to $\pm i\mathbf{M}$, which signifies the critical point of the \mathcal{PT} transition [43]. For $\delta_1 > t_1$, the average spin vector remains aligned with $\pm i\mathbf{M}$, resulting in $S_{\mathcal{PT}}$ -symmetric pairs of spin orbits, where each orbit individually breaks the $S_{\mathcal{PT}}$ symmetry; see Fig. 2(d3).

Summary and outlook.— We have uncovered the physical mechanism governing non-Hermitian spectral properties and symmetry breaking. The intuitive physical picture presented here not only enhances our comprehension of non-Hermitian phenomena but also offers practical insights for their manipulation. This framework operates within the general context of non-Hermitian physics, making it applicable to a wide range of areas in physics, such as quantum physics, condensed

matter physics, optics and acoustics. Demonstrating the quantum-classical correspondence in various physical systems shows great promise by comparing quantum eigenenergies with the corresponding semiclassical dynamics across different parametric regions. Meanwhile, extending the current theory from single-particle to many-body scenarios is also of significant interest.

ACKNOWLEDGMENTS

This work was supported by the National Natural Science Foundation of China (No. 12074172 and No. 12222406), the Natural Science Foundation of Jiangsu Province (No. BK20233001), the Fundamental Research Funds for the Central Universities (No. 2024300415), and the National Key Projects for Research and Development of China (No. 2022YFA120470).

-
- [1] C. M. Bender, Reports on Progress in Physics **70**, 947 (2007).
- [2] Z. G. Yuto Ashida and M. Ueda, Advances in Physics **69**, 249 (2020).
- [3] R. El-Ganainy, K. G. Makris, M. Khajavikhan, Z. H. Musslimani, S. Rotter, and D. N. Christodoulides, Nature Physics **14**, 11 (2018).
- [4] C. M. Bender and S. Boettcher, Phys. Rev. Lett. **80**, 5243 (1998).
- [5] A. Guo, G. J. Salamo, D. Duchesne, R. Morandotti, M. Volatier-Ravat, V. Aimez, G. A. Siviloglou, and D. N. Christodoulides, Phys. Rev. Lett. **103**, 093902 (2009).
- [6] C. E. Rüter, K. G. Makris, R. El-Ganainy, D. N. Christodoulides, M. Segev, and D. Kip, Nature Physics **6**, 192 (2010).
- [7] A. Regensburger, C. Bersch, M.-A. Miri, G. Onishchukov, D. N. Christodoulides, and U. Peschel, Nature **488**, 167 (2012).
- [8] B. Peng, Ş. K. Özdemir, F. Lei, F. Monifi, M. Gianfreda, G. L. Long, S. Fan, F. Nori, C. M. Bender, and L. Yang, Nature Physics **10**, 394 (2014).
- [9] L. Feng, Z. J. Wong, R.-M. Ma, Y. Wang, and X. Zhang, Science **346**, 972 (2014).
- [10] Ş. K. Özdemir, S. Rotter, F. Nori, and L. Yang, Nature materials **18**, 783 (2019).
- [11] L. Feng, Y.-L. Xu, W. S. Fegadolli, M.-H. Lu, J. E. B. Oliveira, V. R. Almeida, Y.-F. Chen, and A. Scherer, Nature Materials **12**, 108 (2013).
- [12] L. Feng, R. El-Ganainy, and L. Ge, Nature Photonics **11**, 752 (2017).
- [13] S. Longhi, Phys. Rev. Lett. **122**, 237601 (2019).
- [14] S. Longhi, Phys. Rev. Res. **1**, 023013 (2019).
- [15] T. E. Lee, F. Reiter, and N. Moiseyev, Phys. Rev. Lett. **113**, 250401 (2014).
- [16] Q. Lin, T. Li, L. Xiao, K. Wang, W. Yi, and P. Xue, Phys. Rev. Lett. **129**, 113601 (2022).
- [17] H. Jiang, L.-J. Lang, C. Yang, S.-L. Zhu, and S. Chen, Phys. Rev. B **100**, 054301 (2019).
- [18] A. Jazaeri and I. I. Satija, Phys. Rev. E **63**, 036222 (2001).
- [19] Y. Liu, Q. Zhou, and S. Chen, Phys. Rev. B **104**, 024201 (2021).
- [20] M.-A. Miri and A. Alù, Science **363**, eaar7709 (2019), <https://www.science.org/doi/pdf/10.1126/science.aar7709>.
- [21] C. Dembowski, B. Dietz, H.-D. Gräf, H. L. Harney, A. Heine, W. D. Heiss, and A. Richter, Phys. Rev. E **69**, 056216 (2004).
- [22] E. J. Bergholtz, J. C. Budich, and F. K. Kunst, Rev. Mod. Phys. **93**, 015005 (2021).
- [23] W. Chen, Ş. K. Özdemir, G. Zhao, J. Wiersig, and L. Yang, Nature **548**, 192 (2017).
- [24] S. Yao and Z. Wang, Phys. Rev. Lett. **121**, 086803 (2018).
- [25] F. K. Kunst, E. Edvardsson, J. C. Budich, and E. J. Bergholtz, Phys. Rev. Lett. **121**, 026808 (2018).
- [26] K. Yokomizo and S. Murakami, Phys. Rev. Lett. **123**, 066404 (2019).
- [27] D. S. Borgnia, A. J. Kruchkov, and R.-J. Slager, Phys. Rev. Lett. **124**, 056802 (2020).
- [28] N. Okuma, K. Kawabata, K. Shiozaki, and M. Sato, Phys. Rev. Lett. **124**, 086801 (2020).
- [29] K. Zhang, Z. Yang, and C. Fang, Phys. Rev. Lett. **125**, 126402 (2020).
- [30] M. Fruchart, R. Hanai, P. B. Littlewood, and V. Vitelli, Nature **592**, 363 (2021).
- [31] J. Wiersig, Phys. Rev. Lett. **112**, 203901 (2014).
- [32] M. Brandenbourger, X. Locsin, E. Lerner, and C. Coullais, Nature Communications **10**, 4608 (2019).
- [33] Z. Dong, Z. Li, F. Yang, C.-W. Qiu, and J. S. Ho, Nature Electronics **2**, 335 (2019).
- [34] W.-T. Xue, M.-R. Li, Y.-M. Hu, F. Song, and Z. Wang, Phys. Rev. B **103**, L241408 (2021).
- [35] Q. Wang, C. Zhu, Y. Wang, B. Zhang, and Y. D. Chong, Phys. Rev. B **106**, 024301 (2022).
- [36] K. Shao, H. Geng, E. Liu, J. L. Lado, W. Chen, and D. Y. Xing, Phys. Rev. Lett. **132**, 156301 (2024).
- [37] H. Geng, J. Y. Wei, M. H. Zou, L. Sheng, W. Chen, and D. Y. Xing, Phys. Rev. B **107**, 035306 (2023).
- [38] A. Mostafazadeh, Journal of Mathematical Physics **43**, 205 (2002).
- [39] E. P. Wigner, Journal of Mathematical Physics **1**, 409

- (1960).
- [40] D. W. McLaughlin, *Journal of Mathematical Physics* **13**, 1099 (1972).
 - [41] K. Shao, Z.-T. Cai, H. Geng, W. Chen, and D. Y. Xing, *Phys. Rev. B* **106**, L081402 (2022).
 - [42] G. Yang, Y.-K. Li, Y. Fu, Z. Wang, and Y. Zhang, *Phys. Rev. B* **109**, 045110 (2024).
 - [43] See Supplemental Material at xxx for the derivations of the restriction on the propagator by η -pseudo-Hermiticity, complex path integral and classical S_η symmetry, non-Hermitian Gutzwiller trace formula, and symmetry of semiclassical orbits and its constraint on energy spectrum, the calculation details of specific examples of continuous systems, and the discussion on \mathcal{PT} transition in two-level systems, which includes Ref. [44, 46–48].
 - [44] M. C. Gutzwiller, *Journal of Mathematical Physics* **12**, 343 (1971).
 - [45] C. M. Bender and S. A. Orszag, *Advanced mathematical methods for scientists and engineers I: Asymptotic methods and perturbation theory* (Springer Science & Business Media, 2013).
 - [46] R. Rajaraman, *Solitons and instantons: An introduction to solitons and instantons in quantum field theory* (North Holland, 1987).
 - [47] H. Nielsen and D. Rohrlich, *Nuclear Physics B* **299**, 471 (1988).
 - [48] A. Altland and B. D. Simons, *Condensed matter field theory* (Cambridge university press, 2010).

End Matter

Appendix.—The second example is the nonreciprocal lattices subject to a magnetic field [41], described by the Hamiltonian $\mathcal{H}_2 = -2[t_0 \cos \hat{p}_x + i\delta_x \sin \hat{p}_x + t_0 \cos(p_y - B\hat{x})]$, where Fourier transform is performed in the y direction with p_y the corresponding momentum and δ_x measures the nonreciprocity of hopping in the x direction. In this way, the Hamiltonian reduces to an effective 1D problem with non-Hermitian skin effect. The magnetic field manifests as a potential modulation, with the dynamics of particle resembling the 1D projection of the cyclotron motion in 2D space. The real energy levels in the long-wavelength limit were explained in Ref. [41], yet an interpretation of the remaining part is still lacking. The 2D system possesses the combined mirror-time reversal symmetry, which can be in-

terpreted as the \mathcal{MT} -PHS: $\mathcal{MT}\mathcal{H}_2(\mathcal{MT})^{-1} = \mathcal{H}_2^\dagger$, where the mirror reflection \mathcal{M} is about the x axis. The spectral properties are dictated by the \mathcal{MT} -PHS and its classical counterpart $S_{\mathcal{MT}}$. To verify this, we adopt the periodic boundary condition in the x direction by choosing a proper magnetic field and compare the energy spectra obtained by two approaches in Fig. 2(b1). The semiclassical 1D Hamiltonian obeys the symmetry $S_{\mathcal{MT}} : H_2(x - p_y/B, -p_x) = H_2^*(x^* - p_y/B, p_x^*)$, where p_y/B is real. It reduces to $H_2(x, -p_x) = H_2^*(x^*, p_x^*)$ through the replacement $x \rightarrow x + p_y/B$. Accordingly, two solutions of $S_{\mathcal{MT}}$ -symmetric orbits $O_1(t) = \{x(t), p_x(t)\}$ and $O_2(t^*) = \{x^*(-t), -p_x^*(-t)\}$ come up in pairs. In particular, the motion of a particle (hole) near the band bottom (top) exhibits $S_{\mathcal{MT}}$ symmetry, giving rise to real Landau levels after quantization; see Fig. 2(b2); However, for energies away from band edges the particle can traverse the potential, resulting in $S_{\mathcal{MT}}$ -symmetric pairs of semiclassical orbits as well as complex eigenvalues, as shown in Fig. 2(b3).

For the third example, we consider a particle moving within a double-well potential that is subject to an antisymmetric gain and loss effect described by the Hamiltonian $\mathcal{H}_3 = \hat{p}^2 + g(\hat{x}^2 - a^2)^2 + i\Gamma\hat{x}$, where g, a, Γ are real parameters. The model possesses \mathcal{PT} symmetry, or equivalently, the \mathcal{PT} -PHS: $\mathcal{PT}\mathcal{H}_3(\mathcal{PT})^{-1} = \mathcal{H}_3^\dagger$. The energy spectrum is shown in Fig. 2(c1), characterized by high-energy real eigenvalues and low-energy complex conjugate pairs. Its semiclassical interpretation is reflected by the symmetry $S_{\mathcal{PT}} : H_3(-x, p) = H_3^*(x^*, p^*)$. Such a constraint by symmetry dictates the equation of motion and leads to two series of solutions $O_1(t) = \{x(t), p(t)\}$ and $O_2(t^*) = \{-x^*(-t), p^*(-t)\}$, which form $S_{\mathcal{PT}}$ -symmetric pairs. At high energies, particles move freely in the whole region and the gain and loss effects compensate each other. Therefore, the orbits possess the $S_{\mathcal{PT}}$ symmetry and the eigenenergies are real after quantization; see Fig. 2(c2). At low energies, however, particles are trapped in the left or right potential wells, experiencing unbalanced gain and loss. As a result, each semiclassical orbit breaks the $S_{\mathcal{PT}}$ symmetry individually, but together they form $S_{\mathcal{PT}}$ -symmetric pairs, as illustrated in Fig. 2(c3).